Bioorganic & Medicinal Chemistry Letters 27 (2017) 3065–3070

Contents lists available at ScienceDirect

Bioorganic & Medicinal Chemistry Letters

journal homepage: www.elsevier.com/locate/bmcl

# Minor phenolics from *Angelica keiskei* and their proliferative effects on Hep3B cells

Yun-Seo Kil [a], Jiyoung Park [a], Mahtab Jafari [b], Hyun Ae Woo [a], Eun Kyoung Seo [a,*]

[a] College of Pharmacy, Graduate School of Pharmaceutical Sciences, Ewha Womans University, Seoul 120-750, Republic of Korea
[b] Department of Pharmaceutical Sciences, University of California, Irvine, CA 92697, United States

ARTICLE INFO

*Article history:*
Received 25 January 2017
Revised 11 May 2017
Accepted 17 May 2017
Available online 18 May 2017

*Keywords:*
Coumarin
Flavonoid
*Angelica keiskei*
Umbelliferae
Cell proliferative effect
Cytoprotective effect

ABSTRACT

A new coumarin, (−)-*cis*-(3′*R*,4′*R*)-4′-*O*-angeloylkhellactone-3′-*O*-β-D-glucopyranoside (**1**) and two new chalcones, 3′-[(2*E*)-5-carboxy-3-methyl-2-pentenyl]-4,2′,4′-trihydroxychalcone (**4**) and (±)-4,2′,4′-trihydroxy-3′-{2-hydroxy-2-[tetrahydro-2-methyl-5-(1-methylethenyl)-2-furanyl]ethyl}chalcone (**5**) were isolated from the aerial parts of *Angelica keiskei* (Umbelliferae), together with six known compounds: (*R*)-*O*-isobutyroyllomatin (**2**), 3′-*O*-methylvaginol (**3**), (−)-jejuchalcone F (**6**), isoliquiritigenin (**7**), davidigenin (**8**), and (±)-liquiritigenin (**9**). The structures of the new compounds were determined by interpretation of their spectroscopic data including 1D and 2D NMR data. All known compounds (**2**, **3**, and **6**–**9**) were isolated as constituents of *A. keiskei* for the first time. To identify novel hepatocyte proliferation inducer for liver regeneration, **1**–**9** were evaluated for their cell proliferative effects using a Hep3B human hepatoma cell line. All isolates exhibited cell proliferative effects compared to untreated control (DMSO). Cytoprotective effects against oxidative stress induced by glucose oxidase were also examined on Hep3B cells and mouse fibroblast NIH3T3 cells and all compounds showed significant dose-dependent protection against oxidative stress.



*Angelica keiskei* ("Shin-Sun Cho" in Korea) is a hardy perennial herb that belongs to the family Umbelliferae.[1] Recent pharmacological studies have provided strong evidences for the curative and preventive effects of *A. keiskei* on obesity,[2] diabetes,[3] hyperlipidemia,[4] hypertension,[5] inflammation,[6] and cancer.[7] Phenolic compounds, in particular chalcones and coumarins, are major components of the herb, which have also been proven to cause the various biological effects.[8–13]

The liver, a vital organ, carries out the majority of the body's detoxification by changing the chemical nature of toxins.[14] For the reason, it is mainly exposed to oxidative stresses and easily damaged by them. Although the liver has a high regenerative capacity, severe or continuous damaging beyond the capacity can prevent complete regeneration and cause an abnormal liver state. According to a patent, orally administrated *A. keiskei* extracts and two major compounds, xanthoangelol and 4-hydroxyderricin, reduced the activities of glutamate oxaloacetate transaminase (GOT) and glutamate pyruvate transaminase (GPT) and induced activities of superoxide dismutase (SOD), catalase, and glutathione peroxidase in rats. The patent emphasized that the hepatoprotective effects of the two compounds were comparable to those of silymarin, a potent liver protector.[15,16] Moreover, a recent clinical study reported that the extracts significantly reduced the levels of gamma-glutamyl transferase (GGT) in heavy alcohol drinkers.[17] In the present phytochemical study on the aerial parts of *A. keiskei*,[18] a new coumarin, (−)-*cis*-(3′*R*,4′*R*)-4′-*O*-angeloylkhellactone-3′-*O*-β-D-glucopyranoside (**1**) and two new chalcones, 3′-[(2*E*)-5-carboxy-3-methyl-2-pentenyl]-4,2′,4′-trihydroxychalcone (**4**) and (±)-4,2′,4′-trihydroxy-3′-{2-hydroxy-2-[tetrahydro-2-methyl-5-(1-methylethenyl)-2-furanyl]ethyl}chalcone (**5**), were isolated from the EtOAc extract together with six known compounds, (*R*)-*O*-isobutyroyllomatin (**2**),[19,20] 3′-*O*-methylvaginol (**3**),[21] (−)-jejuchalcone F (**6**),[22] isoliquiritigenin (**7**),[23] davidigenin (**8**),[24] and (±)-liquiritigenin (**9**)[25] (Fig. 1). All known compounds (**2**, **3**, and **6**–**9**) were identified from *A. keiskei* for the first time. Based on the previous studies, the isolates were expected to promote liver regeneration. Compounds **1**–**9** were evaluated for their cell proliferative effects on the liver using a Hep3B human hepatoma cell line. Cytoprotective effects against oxidative stress induced by glucose oxidase (GOX) were also examined on Hep3B and mouse fibroblast NIH3T3 cells.

Compound **1**[26] was isolated as a colorless, amorphous solid and showed a protonated molecular ion at *m*/*z* 507.1855 (calcd for

* Corresponding author.
*E-mail addresses:* k_yunseo@naver.com (Y.-S. Kil), 37301012@daum.net (J. Park), mjafari@uci.edu (M. Jafari), hawoo@ewha.ac.kr (H.A. Woo), yuny@ewha.ac.kr (E.K. Seo).

http://dx.doi.org/10.1016/j.bmcl.2017.05.054
0960-894X/

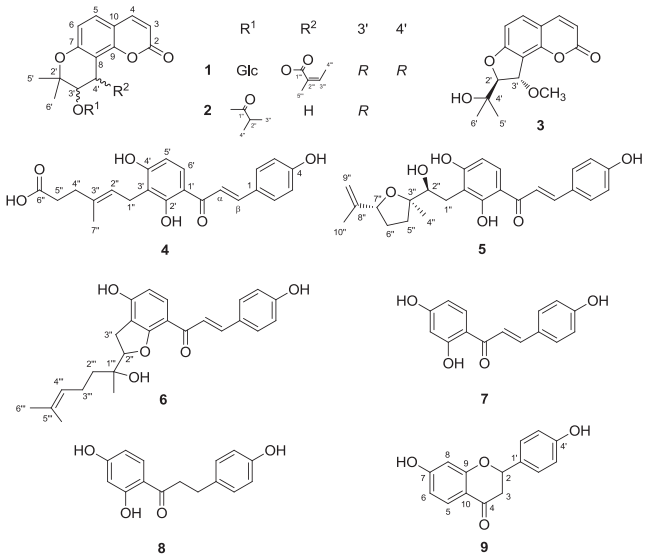

**Fig. 1.** Chemical structures of isolates **1**–**9** from *A. keiskei*.

507.1861) in the HRESIMS, consistent with a molecular formula of $C_{25}H_{30}O_{11}$. The $^1$H and $^{13}$C NMR spectra of **1** exhibited characteristic signals of a khellactone derivative at $\delta_H$ 6.22 (1H, d, $J$ = 9.6 Hz)/$\delta_C$ 113.4 (C-3), 7.85 (1H, d, $J$ = 9.6 Hz)/145.7 (C-4), 7.52 (1H, d, $J$ = 8.8 Hz)/131.1 (C-5), 6.82 (1H, d, $J$ = 8.8 Hz)/115.8 (C-6), 4.44 (1H, d, $J$ = 4.8 Hz)/77.6 (C-3′), 6.74 (1H, d, $J$ = 4.8 Hz)/61.2 (C-4′), 1.56 (3H, s)/27.6 (C-5′), 1.45 (3H, s)/21.5 (C-6′), and $\delta_C$ 162.0 (C-2).[19] Additional signals observed in the $^1$H and $^{13}$C NMR data of **1** were assignable to two other substituents of the khellactone moiety. One was identified as an angeloyl group, signals for which appeared at $\delta_C$ 169.3 (C-1‴), 129.4 (C-2‴), $\delta_H$ 6.06 (1H, qq, $J$ = 7.3, 1.5 Hz)/$\delta_C$ 138.9 (C-3‴), 1.95 (3H, dq, $J$ = 7.3, 1.5 Hz)/16.0 (C-4‴), and 1.85 (3H, quint, $J$ = 1.5 Hz)/20.7 (C-5‴).[27,28] Remaining resonances including a glucosyl anomeric proton signal at $\delta_H$ 4.68 (1H, d, $J$ = 7.6 Hz, H-1″) demonstrated the presence of a β-D-glucopyranosyl unit (Table 1).[29] The HMBC correlation of H-4′ with C-1‴ supported the connectivity of the angeloyl group to C-4′. The β-D-glucopyranosyl unit was assigned at C-3′ by the HMBC correlations of H-3′/C-1″ and H-1″/C-3′ (Fig. 2). The relative *cis*-configuration between C-3′ and C-4′ in **1** was deduced by comparison of the coupling constant ($^3J_{3'4'}$ = 4.8 Hz) with the literature values ($^3J_{3'4'}$ = 4–5 Hz).[27,29,30] Compound **1** was isolated optically active with a specific rotation of $[\alpha]_D^{21}$ −84 (*c* 0.1, MeOH). The absolute configuration of this *cis*-khellactone derivative was determined as "3′*R*,4′*R*" by positive Cotton effects at 301 and 229 nm and a negative Cotton effect at 255 nm in its CD spectrum, which were consistent with those reported for pteryxin [=(+)-*cis*-(3′*R*,4′*R*)-3′-*O*-acetyl-4′-*O*-angeloylkhellactone][31] and (−)-praeruptorin A [=(−)-*cis*-(3′*R*,4′*R*)-4′-*O*-acetyl-3′-*O*-tigloylkhellactone].[30,31] Thus, the structure of **1** was elucidated as the new (−)-*cis*-(3′*R*,4′*R*)-4′-*O*-angeloylkhellactone-3′-*O*-β-D-glucopyranoside.

Compound **4**[26] was obtained as a yellow, amorphous powder, with a molecular formula of $C_{22}H_{22}O_6$ as established by HRESIMS analysis (*m*/*z* 383.1488 $[M+H]^+$, calcd for 383.1489). The $^1$H and $^{13}$C NMR spectra of **4** exhibited the presence of a 3′-substituted chalcone skeleton at $\delta_H$ 7.61 (2H, d, $J$ = 8.6 Hz)/$\delta_C$ 131.8 (C-2 and C-6), 6.84 (2H, d, $J$ = 8.6 Hz)/117.0 (C-3 and C-5), 7.62 (1H, d, $J$ = 15.4 Hz)/118.6 (C-α), 7.78 (1H, d, $J$ = 15.4 Hz)/145.4 (C-β), 6.43 (1H, d, $J$ = 9.0 Hz)/108.3 (C-5′), 7.83 (1H, d, $J$ = 9.0 Hz)/130.5 (C-6′), and $\delta_C$ 193.8 (C=O). The $^1$H and $^{13}$C NMR resonances at $\delta_H$ 3.34 (2H, d, $J$ = 7.2 Hz)/$\delta_C$ 22.5 (C-1″), 5.31 (1H, t, $J$ = 7.2 Hz)/124.1 (C-2″), 2.26 (2H, br t, $J$ = 7.6 Hz)/36.3 (C-4″), 2.33 (2H, br t, $J$ = 7.6 Hz)/34.8 (C-5″), 1.81 (3H, s)/16.2 (C-7″), and $\delta_C$ 178.5 (C-6″), were assignable to a modified geranyl group.[32] A carboxyl C=O group was observed at $\delta_C$ 178.5 (C-6″). The HMBC correlations of $H_2$-4″/C-6″ and $H_2$-5″/C-6″ indicated the position of the C=O group at C-5″ of the modified geranyl group. The C-3′ location of the modified geranyl group on the chalcone skeleton was confirmed by the HMBC correlations of H-1″/C-2′, C-3′, C-4′ (Fig. 2). Therefore, the structure of **4** was elucidated as the new 3′-[(2*E*)-5-carboxy-3-methyl-2-pentenyl]-4,2′,4′-trihydroxychalcone.

Compound **5**[26] was isolated as a yellow, amorphous solid and its molecular formula of $C_{25}H_{28}O_6$ was determined by HRESIMS analysis (*m*/*z* 447.1780 $[M+Na]^+$, calcd for 447.1778). The $^1$H and $^{13}$C NMR spectra of **5** also showed the typical signals for the chalcone skeleton and a methylene group [at $\delta_H$ 3.26 (1H, dd, $J$ = 14.4, 1.9 Hz) and 2.62 (1H, dd, $J$ = 14.4, 9.2 Hz)/$\delta_C$ 26.2 (C-1″)] attached to C-3′, as those of **4**. Remaining $^1$H and $^{13}$C NMR resonances attributed to an exomethylene group [at $\delta_H$ 4.98 and 4.75 (each 1H, br s)/$\delta_C$ 109.9 (C-9″)], two oxygenated methine groups [at $\delta_H$ 4.38 (1H, dd, $J$ = 9.8, 5.8 Hz)/$\delta_C$ 84.1 (C-7″) and 3.82 (1H, dd, $J$ = 9.2, 1.9 Hz)/79.0 (C-2″)], two methylene groups [at $\delta_H$ 2.22 (1H, td, $J$ = 11.5, 7.6 Hz) and 1.68 (1H, ddd, $J$ = 11.5, 7.4, 2.2 Hz)/$\delta_C$ 33.0 (C-5″) and 2.08 and 1.81 (each 1H, m)/32.3 (C-6″)], and two methyl groups [at $\delta_H$ 1.71 (3H, s)/$\delta_C$ 18.1 (C-10″) and 1.33 (3H, s)/23.8 (C-4″)] (Table 1). In the $^{13}$C NMR spectrum, the chemical shifts of C-3″ ($\delta_C$ 86.4) and C-7″ ($\delta_C$ 84.1) suggested the occurrence of a *O*-heterocyclic ring rather than an open side chain containing two OH groups.[33] The $^1$H-$^1$H COSY spectrum of **5** showed correlations of H-1″α/H-2″, H-1″β/H-2″, H-6″α/H-5″β and H-7″, and H-6″β/H-5″α, H-5″β, and H-7″. Moreover, the HMBC cross-peaks of H-2″/C-3″, C-4″, $H_3$-4″/C-3″, C-5″, H-5″β/C-3″, H-6″β/C-3″, H-6″α/C-8″, H-9″a/C-7″, C-8″, C-10″, H-9″b/C-7″, C-10″, and $H_3$-10″/C-7″, C-8″, C-9″ were observed. The observation confirmed the presence of a 2-hydroxy-2-[tetrahydro-2-methyl-5-(1-methylethenyl)-2-furanyl]ethyl moiety.[33] This substituent group was assigned at C-3′ by the HMBC correlations of H-1″α/C-2′, C-3′, C-4′ and H-1″β/C-2′, C-3′, C-4′ (Fig. 2). The relative configuration of **4** is inferred from the $^1$H-$^1$H NOESY NMR spectrum. The $^1$H-$^1$H NOESY NMR spectrum exhibited the key correlations of $H_3$-4″/H-9″a and H-2″ and $H_3$-10″/H-9″b and H-7″ with no correlation between $H_3$-4″ and H-7″ (see Fig. S19, Supplementary Materials). This observation provided evidence that $CH_3$-4″ and H-7″ are on opposite sides of the tetrahydrofuran ring, but H-2″ has the same orientation as $CH_3$-4″. It also demonstrated the geometry of the exomethylene protons in which H-9″a is *trans* and H-9″b is *cis* to $CH_3$-10″.[34] Furthermore, the energy-minimized molecular model of **5** (MM2 of SCIGRESS) with the β-oriented H-7″ (H-2″, $CH_3$-4″: α-oriented) was consistent with the NOESY correlations of H-7″/H-5″β, and H-6″β, H-5″β/H-2″ and H-1″β, H-1″α/$H_3$-4″, and $H_3$-4″/H-5″α and H-6″α. On the basis of the Karplus relationship,[35] the actual coupling constants in the $^1$H NMR spectrum ($^3J_{1''\alpha2''}$ = 1.9 Hz, $^3J_{1''\beta2''}$ = 9.2 Hz, $^3J_{6''\alpha7''}$ = 9.8 Hz, $^3J_{6''\beta7''}$ = 5.8 Hz) were also in accordance with the calculated dihedral angles (Φ) in this molecular model ($\Phi_{1''\alpha2''}$ = 73°, $\Phi_{1''\beta2''}$ = 172°, $\Phi_{6''\alpha7''}$ = 173°, $\Phi_{6''\beta7''}$ = 51°). Compound **5** showed a specific rotation of $[\alpha]_D^{25}$ ± 0 (*c* 0.1, MeOH), which indicated its racemic nature. Thus, the structure of **5** was established as the new compound, (±)-4,2′,4′-trihydroxy-3′-{2-hydroxy-2-[tetrahydro-2-methyl-5-(1-methylethenyl)-2-furanyl]ethyl}chalcone. The structure shown for **5** in Fig. 1 is one of two possible representations with the relative configurations described above.

The liver cell proliferation effects of all compounds were evaluated on human hepatoma Hep3B cells (Table 2).[36,37] Cells were treated with the indicated concentrations of compounds or DMSO alone and cell counts were performed after 4 days of incubation. Daily microscopic examination of the cells showed no differences in cell attachment or morphology between the compound-treated and control cells during the incubation times. As a result, all

**Table 1**
$^{1}$H (400 MHz) and $^{13}$C (100 MHz) NMR spectroscopic data for **1**, **4**, and **5**.[a]

| Position | **1**[b] | | Position | **4**[b] | | **5**[c] | |
|---|---|---|---|---|---|---|---|
| | $\delta_C$ | $\delta_H$ mult ($J$ in Hz) | | $\delta_C$ | $\delta_H$ mult ($J$ in Hz) | $\delta_C$ | $\delta_H$ mult ($J$ in Hz) |
| 2 | 162.0 | | α | 118.6 | 7.62 d (15.4) | 118.5 | 7.79 d (15.4) |
| 3 | 113.4 | 6.22 d (9.6) | β | 145.4 | 7.78 d (15.4) | 145.0 | 7.85 d (15.4) |
| 4 | 145.7 | 7.85 d (9.6) | C=O | 193.8 | | 193.0 | |
| 5 | 131.1 | 7.52 d (8.8) | 1 | 128.0 | | 127.6 | |
| 6 | 115.8 | 6.82 d (8.8) | 2, 6 | 131.8 | 7.61 d (8.6) | 131.8 | 7.75 d (8.6) |
| 7 | 158.3 | | 3, 5 | 117.0 | 6.84 d (8.6) | 116.8 | 6.93 d (8.6) |
| 8 | 109.2 | | 4 | 161.5 | | 161.0 | |
| 9 | 155.4 | | 1′ | 114.6 | | 114.2 | |
| 10 | 113.8 | | 2′ | 165.2 | | 165.3 | |
| 2′ | 79.5 | | 3′ | 116.4 | | 114.8 | |
| 3′ | 77.6 | 4.44 d (4.8) | 4′ | 163.7 | | 165.1 | |
| 4′ | 61.2 | 6.74 d (4.8) | 5′ | 108.3 | 6.43 d (9.0) | 109.6 | 6.47 d (8.8) |
| 5′ | 27.6 | 1.56 s | 6′ | 130.5 | 7.83 d (9.0) | 131.0 | 8.04 d (8.8) |
| 6′ | 21.5 | 1.45 s | 1″ | 22.5 | 3.34 d (7.2) | 26.2 | 3.26 dd (14.4, 1.9, $H_\alpha$)<br>2.62 dd (14.4, 9.2, $H_\beta$) |
| 1″ | 103.1 | 4.68 d (7.6) | 2″ | 124.1 | 5.31 t (7.2) | 79.0 | 3.82 dd (9.2, 1.9) |
| 2″ | 75.6 | 3.18 dd (9.2, 7.6) | 3″ | 134.7 | | 86.4 | |
| 3″ | 78.1 | 3.41 dd (9.2, 8.7) | 4″ | 36.3 | 2.26 br t (7.6) | 23.8 | 1.33 s |
| 4″ | 71.8 | 3.26 dd (9.8, 6.7) | 5″ | 34.8 | 2.33 br t (7.6) | 33.0 | 2.22 td (11.5, 7.6, $H_\beta$)<br>1.67 ddd (11.5, 7.4, 2.2, $H_\alpha$) |
| 5″ | 78.4 | 3.32 m | 6″ | 178.5 | | 32.3 | 2.08 m ($H_\beta$)<br>1.81 m ($H_\alpha$) |
| 6″ | 63.0 | 3.89 dd (11.8, 2.0)<br>3.65 dd (11.8, 2.0) | 7″ | 16.2 | 1.81 s | 84.1 | 4.38 dd (9.8, 5.8) |
| 1‴ | 169.3 | | 8″ | | | 147.4 | |
| 2‴ | 129.4 | | 9″ | | | 109.9 | 4.98 br s<br>4.75 br s |
| 3‴ | 138.9 | 6.06 qq (7.3, 1.5) | 10″ | | | 18.1 | 1.71 s |
| 4‴ | 16.0 | 1.95 dq (7.3, 1.5) | OH-2′ | | | | 14.26 s |
| 5‴ | 20.7 | 1.85 quint (1.5) | | | | | |

[a] TMS was used as internal standard.
[b] Data were measured in methanol-$d_4$.
[c] Data were measured in acetone-$d_6$.

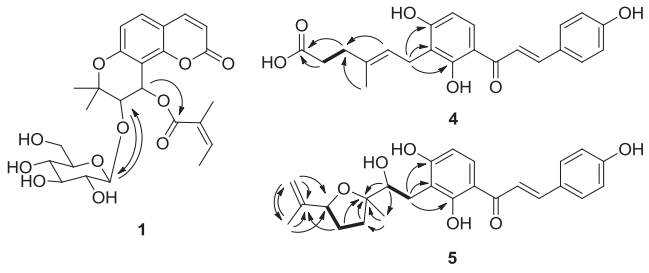


**Fig. 2.** Key $^{1}$H-$^{1}$H COSY (▬) and HMBC (—) correlations of **1**, **4**, and **5**.

compounds promoted growth of hepatoma cells dose-dependently. Among nine compounds, **3** showed the most potent cell proliferative effect. The numbers of Hep3B cells following incubation with 0.1, 1, 10, and 100 μM concentrations of **3** were 105.71, 117.81, 146.75, and 163.03%, respectively ($P < 0.01$ *vs.* control) and compounds **2**, **8**, and **9** also showed a significant growth promotion effect at a concentration of 100 μM (147.43, 140.41, and 134.54%, respectively). Incubation with compounds **1**, and **4**–**7** also led to a significant but smaller dose-dependent liver cell proliferative effect.

Compounds **1**–**9** were evaluated for their cytoprotective effects against oxidative stress in GOX-induced human hepatoma Hep3B cells and mouse fibroblast NIH3T3 cells using MTT assay.[36,38] GOX catalyzed the oxidation of β-D-glucose in the presence of oxygen to produce D-gluconic acid with the simultaneous production of hydrogen peroxide and incubation of the cells with GOX resulted in oxidative damage to the cells.[40] All experiments included GOX-untreated cells, negative controls that were treated with GOX only, and GOX-treated cells that also received the antioxidant

**Table 2**
Cell proliferative effects of **1**–**9** on Hep3B cells.

| Compounds | Viable cells (%) | | | | |
|---|---|---|---|---|---|
| | 0 μM | 0.1 μM | 1 μM | 10 μM | 100 μM |
| **1** | 100 ± 1.52 | 100.55 ± 0.12 | 101.98 ± 1.55 | 112.61 ± 1.71* | 114.19 ± 1.74* |
| **2** | | 100.08 ± 1.12 | 101.30 ± 1.67 | 110.34 ± 1.68* | 147.43 ± 2.24* |
| **3** | | 105.71 ± 0.85* | 117.81 ± 1.79* | 146.75 ± 2.23* | 163.03 ± 2.48* |
| **4** | | 99.98 ± 1.03 | 100.03 ± 1.41 | 107.41 ± 1.63* | 114.77 ± 1.76* |
| **5** | | 100.11 ± 1.21 | 101.10 ± 1.50 | 102.20 ± 1.55* | 115.77 ± 1.66* |
| **6** | | 100.02 ± 0.08 | 101.53 ± 1.54 | 104.24 ± 1.59* | 112.61 ± 1.71* |
| **7** | | 101.12 ± 1.74 | 102.88 ± 1.57 | 108.99 ± 1.66* | 126.17 ± 1.92* |
| **8** | | 103.82 ± 1.95* | 105.82 ± 1.61* | 115.77 ± 1.76* | 140.41 ± 2.14* |
| **9** | | 100.18 ± 1.13 | 103.79 ± 1.58* | 111.93 ± 1.70* | 134.54 ± 2.05* |

* $p < 0.01$ vs. 0 μM group.

**Table 3**
Cytoprotective effects of **1**–**9** against oxidative stress induced by glucose oxidase (GOX) on Hep3B cells (top) and NIH3T3 cells (bottom).

| Hep3B | Viable cells (%) | | | | | |
|---|---|---|---|---|---|---|
| | GOX (15 mU/ml) | | | | | |
| | – | + | + | + | + | + |
| Compounds | 0 μM | 0 μM | 0.1 μM | 1 μM | 10 μM | 100 μM |
| α-Tocopherol[a] | 100.00 ± 1.23 | 41.51 ± 1.39 | 62.22 ± 0.09* | 66.80 ± 0.42* | 70.66 ± 0.03* | 79.58 ± 0.35* |
| **1** | | | 59.24 ± 0.08*# | 65.35 ± 0.39*# | 76.93 ± 0.37*# | 91.24 ± 1.34*# |
| **2** | | | 44.77 ± 1.37 | 56.11 ± 1.04*# | 66.48 ± 1.61*# | 82.32 ± 0.31*# |
| **3** | | | 69.21 ± 1.57*# | 87.06 ± 0.66*# | 100.24 ± 0.85*# | 112.30 ± 1.43*# |
| **4** | | | 44.31 ± 0.39 | 45.50 ± 1.45* | 57.15 ± 0.34*# | 74.12 ± 1.59*# |
| **5** | | | 45.18 ± 1.60* | 60.45 ± 1.32*# | 65.43 ± 1.32*# | 76.77 ± 1.16*# |
| **6** | | | 42.93 ± 1.25 | 48.95 ± 1.04* | 62.14 ± 1.02*# | 75.96 ± 1.44*# |
| **7** | | | 41.88 ± 1.38 | 62.94 ± 1.34*# | 66.16 ± 1.03*# | 75.32 ± 0.37*# |
| **8** | | | 59.32 ± 1.35*# | 83.44 ± 1.67*# | 94.94 ± 0.38*# | 103.70 ± 1.81*# |
| **9** | | | 70.66 ± 1.52*# | 88.42 ± 1.30*# | 98.79 ± 0.97*# | 112.22 ± 1.48*# |
| NIH3T3 | Viable cells (%) | | | | | |
| | GOX (15 mU/ml) | | | | | |
| | – | + | + | + | + | + |
| Compounds | 0 μM | 0 μM | 0.1 μM | 1 μM | 10 μM | 100 μM |
| α-Tocopherol[a] | 100.00 ± 1.08 | 42.71 ± 2.10 | 61.18 ± 0.02* | 65.78 ± 1.13* | 69.06 ± 1.21* | 77.89 ± 0.11* |
| **1** | | | 58.64 ± 0.40*# | 64.46 ± 1.72*# | 75.76 ± 1.02*# | 93.79 ± 2.81*# |
| **2** | | | 45.72 ± 1.56* | 55.60 ± 0.90*# | 67.43 ± 1.11*# | 83.14 ± 1.46*# |
| **3** | | | 69.02 ± 2.18*# | 93.01 ± 3.43*# | 118.12 ± 1.15*# | 128.66 ± 2.25*# |
| **4** | | | 43.25 ± 1.24 | 44.66 ± 0.59 | 57.75 ± 0.99*# | 74.45 ± 0.76*# |
| **5** | | | 44.93 ± 1.38 | 61.42 ± 1.50*# | 66.40 ± 2.09*# | 81.85 ± 1.80*# |
| **6** | | | 43.51 ± 0.93 | 44.40 ± 0.51* | 57.49 ± 1.11*# | 77.76 ± 1.32*# |
| **7** | | | 44.77 ± 0.63 | 59.17 ± 0.72*# | 71.89 ± 0.83*# | 82.94 ± 1.76*# |
| **8** | | | 60.63 ± 0.83*# | 84.04 ± 0.98*# | 113.10 ± 1.54*# | 122.68 ± 1.39*# |
| **9** | | | 74.14 ± 1.42*# | 88.44 ± 2.02*# | 110.70 ± 1.76*# | 125.52 ± 3.28*# |

[a] Positive control.
* $p < 0.01$ vs. 0 μM group.
# $p < 0.01$ vs. positive control.

**Table 4**
Determination of LDH cytotoxicity of **1**–**9** in Hep3B (top) and NIH3T3 cells (bottom).

| Hep3B | LDH Cytotoxicity (%) | | | | | |
|---|---|---|---|---|---|---|
| | GOX (15 mU/ml) | | | | | |
| | – | + | + | + | + | + |
| Compounds | 100 μM | 0 μM | 0.1 μM | 1 μM | 10 μM | 100 μM |
| α-Tocopherol[a] | 3.82 ± 1.35* | 60.94 ± 1.18 | 25.13 ± 1.69* | 21.14 ± 0.82* | 18.89 ± 1.78* | 13.00 ± 1.47* |
| **1** | 2.95 ± 1.02*# | | 28.01 ± 0.82* | 19.57 ± 0.73*# | 10.28 ± 1.62*# | 6.16 ± 1.45*# |
| **2** | 2.46 ± 1.12*# | | 28.99 ± 0.93* | 23.78 ± 1.32*# | 18.04 ± 0.72* | 7.64 ± 1.46*# |
| **3** | 1.61 ± 1.68*# | | 14.07 ± 1.68*# | 10.56 ± 0.78*# | 5.66 ± 1.40*# | 2.59 ± 1.71*# |
| **4** | 3.07 ± 1.55* | | 30.97 ± 0.95* | 20.34 ± 1.08* | 16.93 ± 0.81*# | 7.60 ± 1.39*# |
| **5** | 3.73 ± 1.43* | | 26.09 ± 1.26* | 20.91 ± 0.99* | 14.03 ± 1.78*# | 6.99 ± 0.88*# |
| **6** | 2.21 ± 1.29*# | | 25.13 ± 1.13* | 19.53 ± 1.38*# | 19.08 ± 0.83* | 8.14 ± 1.67*# |
| **7** | 1.74 ± 0.85*# | | 27.14 ± 1.47* | 24.29 ± 0.93* | 21.06 ± 1.79* | 10.10 ± 1.52*# |
| **8** | 3.34 ± 1.61* | | 22.37 ± 1.92*# | 18.61 ± 0.79*# | 11.83 ± 1.56*# | 4.16 ± 1.60*# |
| **9** | 2.64 ± 0.95*# | | 11.57 ± 1.72*# | 6.83 ± 1.51*# | 4.93 ± 1.49*# | 3.82 ± 1.54*# |
| NIH3T3 | LDH Cytotoxicity (%) | | | | | |
| | GOX (15 mU/ml) | | | | | |
| | – | + | + | + | + | + |
| Compounds | 100 μM | 0 μM | 0.1 μM | 1 μM | 10 μM | 100 μM |
| α-Tocopherol[a] | 3.84 ± 1.57* | 63.34 ± 1.85 | 26.51 ± 1.02* | 22.37 ± 1.54* | 15.02 ± 0.73* | 10.51 ± 1.10* |
| **1** | 3.01 ± 1.35*# | | 29.90 ± 0.92* | 21.12 ± 1.51*# | 9.25 ± 1.71*# | 5.75 ± 1.23*# |
| **2** | 2.56 ± 1.17*# | | 31.31 ± 1.49* | 25.89 ± 1.41* | 19.53 ± 1.76* | 8.13 ± 0.60*# |
| **3** | 1.67 ± 1.68*# | | 15.41 ± 1.37*# | 6.59 ± 1.86*# | 4.20 ± 1.40*# | 1.89 ± 1.54*# |
| **4** | 4.24 ± 1.16* | | 36.37 ± 0.71* | 20.71 ± 0.99*# | 18.78 ± 1.11* | 6.96 ± 0.70*# |
| **5** | 3.88 ± 1.42* | | 28.31 ± 0.81* | 20.91 ± 1.17*# | 15.76 ± 1.49* | 6.22 ± 1.71*# |
| **6** | 2.30 ± 1.13*# | | 27.70 ± 0.66* | 21.87 ± 1.33*# | 15.00 ± 1.24* | 12.35 ± 1.27* |
| **7** | 1.18 ± 1.12*# | | 44.26 ± 1.26* | 26.03 ± 1.43* | 22.67 ± 1.85* | 8.85 ± 1.81*# |
| **8** | 5.56 ± 1.18* | | 24.04 ± 1.47*# | 15.74 ± 0.84*# | 12.69 ± 1.28*# | 3.10 ± 1.37*# |
| **9** | 2.75 ± 1.54*# | | 18.42 ± 1.38*# | 7.85 ± 1.27*# | 5.51 ± 0.55*# | 2.63 ± 1.40*# |

[a] Positive control.
* $p < 0.01$ vs. 0 μM group.
# $p < 0.01$ vs. positive control.

α-tocopherol as a positive control. Table 3 shows that the exposure of the cells to 15 mU/ml GOX for 5 h resulted in significant cell death with 41.51% cell survival. All compounds exhibited significant dose-dependent protection against oxidative stress ($P < 0.01$). Compounds **3**, **8**, and **9** showed relatively high activities at concentrations of 0.1, 1, 10, and 100 μM compared with other compounds and their cytoprotective activities were significantly greater than that of the positive control. In addition, incubation with 100 μM **3**, **8**, and **9** promoted proliferation of Hep3B cells with cell viability of 112.30 ± 1.43, 103.70 ± 1.81, and 112.22 ± 1.48%, respectively. Compounds **3**, **8** and **9** also possessed proliferative effects on fibroblast growth and these effects may be related to preventing oxidative stress during cell culture. Moreover, the compounds protected not only Hep3B cells but also NIH3T3 cells against oxidative stress, which infers that the cytoprotective activities of these compounds are not limited to one type of cells. The cytoprotective effects of **1**–**9** against oxidative stress were also investigated using an LDH cytotoxicity assay in Hep3B and NIH3T3 cells.[39,40] The cytotoxicity of Hep3B cells was markedly increased after GOX treatment with 60.94 ± 1.18% LDH cytotoxicity, although this cytotoxicity was ameliorated in a dose-dependent manner by incubation with all compounds (Table 4). Compounds **3**, **8** and **9** showed the most potent protective effects decreasing the cytotoxicity to 2.59 ± 1.71, 4.16 ± 1.60, and 3.82 ± 1.54% at 100 μM, respectively. The cytoprotective effect of all compounds in NIH3T3 cells was similar to that of Hep3B cells (Table 4).

The overall bioassay results suggested that **3**, **8**, and **9** are proliferative compounds in human hepatoma Hep3B cells with cytoprotective effects. Among coumarins (**1**–**3**), the furanocoumarin (**3**) was more potent than the pyranocoumarins (**1** and **2**). This might propose that the presence of the furan ring fused at C7-C8 of the coumarin skeleton is related to the potency. However, because of the differences in the substituted groups, further research is needed to support this finding. The chalcone compound with no substituent group at C-3′ (**7**) showed the cell proliferative activity higher than other chalcones with different substituent groups at C-3′ (**4**–**6**). There was no significant difference between these chalcones (**4**–**7**) in the cytoprotective activities. When considering only the simple flavonoids (**7**–**9**) for the bioactivities, the dihydrochalcone (**8**) and the flavanone (**9**) were more active than the chalcone (**7**).

## Acknowledgments

This research is supported by Ewha Womans University (collaborative research grant for Ewha-UC Irvine).

## A. Supplementary data

Supplementary data associated with this article can be found, in the online version, at http://dx.doi.org/10.1016/j.bmcl.2017.05.054.

## References


1. Sarker SD, Nahar L. *Curr Med Chem*. 2004;11:1479–1500.
2. Zhang T, Yamashita Y, Yasuda M, Yamamoto N, Ashida H. *Food Funct*. 2015;6:134–145.
3. Ohnogi H, Hayami S, Kudo Y, et al. *Biosci Biotechnol Biochem*. 2012;76:928–932.
4. Kim E, Choi J, Yeo I. *Nutr Res Pract*. 2012;6:9–15.
5. Shimizu E, Hayashi A, Takahashi R, Aoyagi Y, Murakami T, Kimoto K. *J Nutr Sci Vitaminol*. 1999;45:375–383.
6. Lee HJ, Choi TW, Kim HJ, et al. *J Med Food*. 2010;13:691–699.
7. Jeong Y-J, Kang KJ. *J Korean Soc Food Sci Nutr*. 2011;40:1654–1661.
8. Enoki T, Ohnogi H, Nagamine K, et al. *J Agric Food Chem*. 2007;55:6013–6017.
9. Akihisa T, Kikuchi T, Nagai H, Ishii K, Tabata K, Suzuki T. *J Oleo Sci*. 2011;60:71–77.
10. Takaoka S, Hibasami H, Ogasawara K, Imai N. *J Herbs Spices Med Plants*. 2008;14:166–174.
11. Zhang T, Sawada K, Yamamoto N, Ashida H. *Mol Nutr Food Res*. 2013;57:1729–1740.
12. Ogawa H, Nakamura R, Baba K. *Clin Exp Pharmacol Physiol*. 2005;32:1104–1109.
13. Ogawa H, Ohno M, Baba K. *Clin Exp Pharmacol Physiol*. 2005;31:19–23.
14. Michalopoulos GK. *J Cell Physiol*. 2007;213:286–300.
15. Kim TS, Shim JS, Kim SD, Yeo IH. Application: KR: (Pulmuone Co., Ltd, S. Korea); 2006.
16. Feher J, Lengyel G. *Curr Pharm Biotechnol*. 2012;13:210–217.
17. Noh H-M, Ahn E-M, Yun J-M, Cho B-L, Paek Y-J. *J Med Food*. 2015;18:166–172.
18. *Plant materials:* The aerial parts of *A. keiskei* were purchased from the Chodamchae in Seoul, Korea and identified by Professor Je-hyun Lee (College of Oriental Medicine, Dongguk University). A voucher specimen (no. EA327) has been deposited at the Natural Product Chemistry Laboratory, College of Pharmacy, Ewha Womans University. *Extraction and isolation:* The aerial parts of *A. keiskei* (8 kg) were extracted with MeOH (2 × 12 l) at room temperature overnight. The solvent was evaporated under reduced pressure to afford 2.5 kg of a concentrated MeOH extract. The crude extract was suspended in MeOH-$H_2O$ (19:1, 4 l) mixture and then fractionated with hexanes (5 × 4 l). The concentrated MeOH-$H_2O$-soluble extract was suspended in distilled water and partitioned with EtOAc (5 × 4 l). The EtOAc (142 g) was chromatographed over silica gel by elution with gradient mixtures of hexanes-EtOAc (99:1 → 1:1) and EtOAc-MeOH (1:0 → 0:1) to afford 16 fractions (Fr. 01-Fr. 16). Fr. 05 (2 g) was subjected to RP-18 CC, eluted by a MeOH-$H_2O$ gradient solvent system (2:3 → 4:1) to yield **2** (18.9 mg, $2.36 \times 10^{-3}$%*w/w*). Fr. 07 (7 g) was chromatographed over silica gel using gradient mixtures of $CHCl_3$-MeOH (199:1 → 9:1) to obtain 18 subfractions (Fr. 07.01-Fr. 07.18). Fr. 07.18 (45 mg) was purified by Sephadex LH-20 CC with MeOH 100% as eluent to yield **10** (3.1 mg, $3.9 \times 10^{-5}$% *w/w*). Fr. 11 (14 g) was chromatographed over silica gel using a $CHCl_3$-MeOH gradient solvent system (199:1 → 4:1) to yield 16 subfractions (Fr. 11.01-Fr. 11.16). Fr. 11.12 (9 g) was subjected to RP-18 CC, eluted by gradient solvent mixtures of MeOH-$H_2O$ (2:3 → 4:1) to obtain 22 subfractions (Fr. 11.12.01-Fr. 11.12.22). Compound **3** (8.6 mg, $1.0 \times 10^{-4}$%*w/w*) was separated from Fr. 11.12.07 (64 mg) by RP-18 CC using MeOH-$H_2O$ (1:1) as eluent. Fr. 11.12.16 (262 mg) was subjected to RP-18 CC by elution with MeOH-$H_2O$ (4:1) and then purified by separation over Sephadex LH-20 CC with MeOH 100%, to yield **5** (4.2 mg, $5.2 \times 10^{-5}$%*w/w*). Fr. 11.15 (1 g) was subjected to RP-18 CC (MeOH-$H_2O$ = 1:1 → 7:3), providing 15 subfractions (Fr. 11.15.01-Fr. 11.15.15). Fr. 11.15.03 (3 mg), Fr. 11.15.06 (6 mg), and Fr. 11.15.07 (12 mg) were separately chromatographed over Sephadex LH-20 using MeOH 100%, resulting in the purification of **9** (1.0 mg, $1.3 \times 10^{-5}$%*w/w*), **8** (1.6 mg, $2.0 \times 10^{-5}$%*w/w*), and **7** (4.1 mg, $1.3 \times 10^{-5}$%*w/w*), respectively. Fr. 13 (3 g) was chromatographed over silica gel, eluted by gradient solvent mixtures of $CHCl_3$-acetone (49:1 → 4:1) to obtain 21 subfractions (Fr. 13.01-Fr. 13.21). Fr. 13.20 (528 mg) was subjected to RP-18 CC using a MeOH-$H_2O$ gradient solvent system (2:3 → 9:1) to give 24 subfractions (Fr. 13.20.01-Fr. 13.20.24). Fr. 13.20.17 (16 mg) was further purified by separation over Sephadex LH-20 CC using MeOH 100% as eluent, to yield **6** (9.4 mg, $1.2 \times 10^{-4}$%*w/w*). Fr. 15 (25 g) was chromatographed over silica gel by elution with gradient mixtures of $CHCl_3$-MeOH (99:1 → 9:1) and $CHCl_3$-MeOH-$H_2O$ (90:10:1 → 15:10:2) to obtain 12 subfractions (Fr. 15.01-Fr. 15.12). Fr. 15.12 (9 g) was subjected to RP-18 CC with MeOH-$H_2O$ (2:3 → 4:1) as a gradient solvent system to give 17 subfractions (Fr. 15.12.01-Fr. 15.12.21). Compounds **1** (2.8 mg, $3.5 \times 10^{-5}$%*w/w*) and **4** (2.7 mg, $3.4 \times 10^{-5}$%*w/w*) were separated from the Fr. 15.12.10 (60 mg) and Fr. 15.12.19 (51 mg) by Sephadex LH-20 CC using MeOH 100%, respectively.
19. Valencia-Islas N, Abbas H, Bye R, Toscano R, Mata R. *J Nat Prod*. 2002;65:828–834.
20. Buendia-Trujillo AI, Torrres-Valencia JM, Joseph-Nathan P, Burgueno-Tapia E. *Tetrahedron: Asymmetry*. 2014;25:1418–1423.
21. Chang C-I, Hu W-C, Shen C-P, et al. *Int J Mol Sci*. 2014;15:4608–4618.
22. Shimomura K, Sugiyama Y, Nakamura J, Ahn M-R, Kumazawa S. *Phytochemistry*. 2013;93:222–229.
23. Yahara S, Ogata T, Saijo R, et al. *Chem Pharm Bull*. 1989;37:979–987.
24. Chen H-J, Chung C-P, Chiang W, Lin Y-L. *Food Chem*. 2011;126:1741–1748.
25. Kulesh NI, Vasilevskaya NA, Veselova MV, Denisenko VA, Fedoreev SA. *Chem Nat Compd*. 2008;44:712–714.
26. *Physical and spectroscopic data of new compounds:* (−)-*cis-(3′R,4′R)-4′-O-angeloylkhellactone-3′-O-β-D-glucopyranoside* (**1**): colorless amorphous solid; $[\alpha]_D^{21}$ −84 (*c* 0.1, MeOH); UV (MeOH) $\lambda_{max}$ (log $\varepsilon$) 325 (4.05), 298 (3.85), 257 (3.67), 220 (4.28) nm; CD (*c* 0.2 mM, MeOH) $\Delta\varepsilon$ (nm) +0.83 (301), −3.29 (255), +9.18 (229); $^1$H and $^{13}$C NMR data, see Table 1; HRESIMS *m/z* 507.1855 $[M+H]^+$ (calcd for $C_{25}H_{31}O_{11}$, 507.1861). *3′-[(2E)-5-carboxy-3-methyl-2-pentenyl]-4,2′,4′-trihydroxychalcone* (**4**): yellow amorphous powder; UV (MeOH) $\lambda_{max}$ (log $\varepsilon$) 367 (4.18), 228 (4.01) nm; $^1$H and $^{13}$C NMR data, see Table 1; HRESIMS *m/z* 383.1488 $[M+H]^+$ (calcd for $C_{22}H_{23}O_6$, 383.1489). *(±)-4,2′,4′-Trihydroxy-3′-{2-hydroxy-2-[tetrahydro-2-methyl-5-(1-methylethenyl)-2-furanyl]ethyl}chalcone* (**5**): yellow amorphous powder; $[\alpha]_D^{25}$ ±0 (*c* 0.1, MeOH); UV (MeOH) $\lambda_{max}$ (log $\varepsilon$) 370 (4.47) nm; $^1$H and $^{13}$C NMR data, see Table 1; HRESIMS *m/z* 447.1780 $[M+Na]^+$ (calcd for $C_{25}H_{28}O_6Na$, 447.1778).
27. Chen I-S, Chang C-T, Sheen W-S, et al. *Phytochemistry*. 1996;41:525–530.
28. Song Y-L, Jing W-H, Chen Y-G, Yuan Y-F, Yan R, Wang Y-T. *J Pharm Biomed Anal*. 2014;93:86–94.
29. Hisamoto M, Kikuzaki H, Ohigashi H, Nakatani N. *J Agric Food Chem*. 2003;51:5255–5261.
30. Xu Z, Wang X, Dai Y, et al. *Chem Biol Interact*. 2010;186:239–246.
31. Lou H-X, Sun L-R, Yu W-T, et al. *J Asian Nat Prod Res*. 2004;6:177–184.
32. Kil Y-S, Choi S-K, Lee Y-S, Jafari M, Seo E-K. *J Nat Prod*. 2015;78:2481–2487.

33. Navratilova A, Schneiderova K, Vesela D, et al. *Phytochemistry*. 2013;89:104–113.
34. Ma J, Pawar RS, Grundel E, et al. *J Nat Prod*. 2015;78:315–319.
35. Pavia DL, Lampman GM, Kriz GS. *Introduction to spectroscopy: a guide for students of organic chemistry*. 3rd ed. Philadelphia: Harcourt College Publishing; 2001.
36. *Cell Culture:* The Hep3B human liver cancer and mouse fibroblasts NIH3T3 cells were obtained from American Type Culture Collection (Manassas, VA, USA). The NIH3T3 cells appeared fibroblastic morphology and Hep3B cells were polygonal. Both cells were tightly adherent to the flask, and were highly proliferative. NIH3T3 cells were cultured in Dulbecco's Modified Eagle's Medium (DMEM, Welgene, Korea) supplemented with 10% bovine calf serum (HyClone) and 1% penicillin-streptomycin (HyClone), Hep3B cells were maintained in DMEM supplemented with 10% fetal bovine serum (HyClone) and 1% penicillin-streptomycin. Cells were maintained at 37°C with 5% $CO_2$ in a humidified atmosphere. The cells were subcultured when 80% confluence was reached according to the manufacturer's recommendation. The morphology of the cells was examined under a microscope.
37. *Cell Proliferation Assay:* Cell number count was conducted in monolayer culture in 12-well. For the dose-dependency of cell proliferative effects of compounds, Hep3B cells were seeded at an initial density of $1 \times 10^5$ cells per ml medium containing **1**–**10** (0.1–100 μM, control DMSO only) and the effect on cell growth was determined after 4 days by counting cell numbers. Cell numbers were counted in triplicate for each group, and three independent experiments were performed.
38. *Cytoprotection Assay against oxidative stress induced by GOX:* Cell viability was measured by methyl thiazol tetrazolium (MTT) assay. This is a colorimetric assay that measures the reduction of yellow 3-(4,5-dimethythiazol- 2-yl)-2,5-diphenyl tetrazolium bromide (MTT) by mitochondrial succinate dehydrogenase. The MTT enters the cells and passes into the mitochondria where it is reduced to an insoluble, coloured (dark purple) formazan product. The cells are then solubilised with an organic solvent and the released, solubilised formazan reagent is measured spectrophotometrically. Since reduction of MTT can only occur in metabolically active cells the level of activity is a measure of the viability of the cells. Cells were seeded in 48-well plates at a density of $7 \times 10^4$ cells/well. On the next day, cells were treated with indicated concentrations of α-tocopherol or compounds and 15 mU/ml GOX (Sigma-Aldrich) in growth media for 5 h and then, cells were gently washed twice with growth medium and incubated with 0.5mg/ml MTT (Sigma-Aldrich) at 37°C for an hour. After this incubation period, purple formazan salt crystals are formed. The formazan crystals formed by active mitochondria were dissolved in DMSO and $A_{540}$ for each well was measured with spectrophotometer. The solubilized formazan product is spectrophotometrically quantified using an spectrophotometer. An increase in number of living cells results in an increase in the total metabolic activity in the sample. This increase directly correlates to the amount of purple formazan crystals formed, as monitored by the absorbance.
39. *LDH leakage assay:* GOX-mediated cytotoxicity was measured by LDH assay. Lactate dehydrogenase (LDH) is a cytosolic enzyme present in many different cell types. Plasma membrane damage releases LDH into the cell culture media. Extracellular LDH in the media can be quantified by a coupled enzymatic reaction in which LDH catalyzes the conversion of lactate to pyruvate via NAD+ reduction to NADH. Diaphorase then uses NADH to reduce a tetrazolium salt (INT) to a red formazan product that can be measured at 490 nm. The level of formazan formation is directly proportional to the amount of LDH released into the medium, which is indicative of cytotoxicity. Cells were seeded in 96-well plates at a density of $4.5 \times 10^4$ cells/well. On the next day, cells were treated with indicated concentrations of α-tocopherol or compounds and 15 mU/ml GOX (Sigma-Aldrich) in growth media for 5 h. Cultured cells were incubated compounds to induced cytotoxicity and subsequently release LDH. The LDH released into the media is transferred to a new plate and mixed with Reaction Mixture (Pierce LDH Cytotoxicity Assay Kit). After a 30 min room temperature incubation, reactions are stopped by adding Stop Solution (Pierce LDH Cytotoxicity Assay Kit). Absorbance at 490 nm and 680 nm is measured using a plate-reading spectrophotometer to determine LDH activity. To determine LDH activity, the 680 nm absorbance value (background) was subtracted from the 490 nm absorbance before calculation of % Cytotoxicity [(LDH at 490 nm) − (LDH at 680 nm)]. To calculate % Cytotoxicity, the LDH activity of the Spontaneous LDH Release Control (water-treated) was subtracted from the chemical-treated sample LDH activity, and then was divided by the total LDH activity [(Maximum LDH Release Control activity) − (Spontaneous LDH Release Control activity)].
40. Kang U, Park J, Han A-R, et al. *Arch Pharm Res*. 2016;39:474–480.